Structural Engineering and Mechanics, Vol. 40, No. 5 (2011) 719-743
DOI: http://dx.doi.org/10.12989/sem.2011.40.5.719

Hybrid damage monitoring of steel plate-girder bridge under train-induced excitation by parallel acceleration-impedance approach

D.S. Hong[1a], H.J. Jung[2b] and J.T. Kim*[1]

[1]*Department of Ocean Eng, Pukyong National University, Nam-gu, Busan 608-737, Korea*
[2]*Department of Civil and Environmental Eng., Korea Advanced Institute Science and Technology, Daejeon, Korea*

(Received September 20, 2010, Revised July 15, 2011, Accepted October 27, 2011)

Abstract. A hybrid damage monitoring scheme using parallel acceleration-impedance approaches is proposed to detect girder damage and support damage in steel plate-girder bridges which are under ambient train-induced excitations. The hybrid scheme consists of three phases: global and local damage monitoring in parallel manner, damage occurrence alarming and local damage identification, and detailed damage estimation. In the first phase, damage occurrence in a structure is globally monitored by changes in vibration features and, at the same moment, damage occurrence in local critical members is monitored by changes in impedance features. In the second phase, the occurrence of damage is alarmed and the type of damage is locally identified by recognizing patterns of vibration and impedance features. In the final phase, the location and severity of the locally identified damage are estimated by using modal strain energy-based damage index methods. The feasibility of the proposed scheme is evaluated on a steel plate-girder bridge model which was experimentally tested under model train-induced excitations. Acceleration responses and electro-mechanical impedance signatures were measured for several damage scenarios of girder damage and support damage.

Keywords: acceleration; impedance; hybrid; structural health monitoring; steel plate-girder; girder crack; support failure

1. Introduction

A structure suffers a history of damage events during its life cycle. By monitoring critical damages at its early stage, the structural safety and integrity will be guaranteed and, at the same time, the time and cost associated with proper maintenance and repair will be greatly reduced. As the concern goes to railway bridges, structural health monitoring (SHM) is required to guarantee the serviceability of the structures. For a steel plate-girder bridge under train-induced dynamic loadings, structural properties in girders and reaction capacities in supports are two important parameters that should be secured for its safety. If not monitored in timely manner, the damages occurred in those

*Corresponding author, Professor, E-mail: idis@pknu.ac.kr
[a]Postdoctoral Research
[b]Professor

critical subsystems may result in tragic collapse of the structure.

Since as early as 1970s, many researchers have focused on the use of vibration characteristics of a structure as an indication of its structural damage (Adams *et al*. 1978, Stubbs and Osegueda 1990). The most appealing features using vibration characteristics are simplicity in measurement and promptness in global diagnosis. Thus, many researchers have made efforts to develop robust vibration-based techniques that can be implemented for global SHM practices in structures. Recently, research efforts have been focused on searching for suitable sensitive-to-damage vibration features such as mode shape-curvature, modal sensitivity, modal strain-energy, and modal flexibility (Doebling *et al*. 1998, Gao and Spencer 2002, Kim *et al*. 2003, Catbas *et al*. 2006).

The vibration-based global SHM relies very much on acceleration responses of low frequency range. This activity includes detecting, locating, and identifying damage by measuring vibration responses of the entire structure. Those vibration responses represent global motions which react to any changes in the structure. However, they are not sensitive enough to detect small localized damage, such as incipient cracks or minor changes in support systems (Sohn *et al*. 2003). Also, those acceleration-based approaches may not easily distinguish multiple damage-types (e.g., girder crack and support failure) since the monitored change in vibration characteristics may be attributed to any damage-types. Even significant damage in critical members may cause relatively small changes in vibration responses, particularly for large complex structures. Moreover, those small changes may not be recognized as structural damage due to uncertainties in environmental and operational conditions (Yang *et al*. 1997, Ni *et al*. 2005, Kim *et al*. 2007).

Since the global SHM covers the entire structure, the sensors are generally distributed on overall structure with a large interval. Thus, the distributed density of the sensors is low, and the detailed local damage information in the obtained dynamic response would not be enough to judge the local damage state. Naturally, local health monitoring has grabbed the demand. Recently, the electro-mechanical impedance technique has emerged as a valuable local SHM tool and implemented on several complex structures to detect incipient-type damage such as small cracks or loose connections at local points (Kessler 2002, Giurgiutiu and Zagrai 2002, Bhalla and Soh 2004, Park *et al*. 2005, Park *et al*. 2006). Compared to vibration-based approaches, the impedance-based method has the capability of more precisely locating damage on small scale. In this technique, a PZT patch is attached to the structure and a series of impedance signatures are sensed to make a diagnosis of the structure.

However, there are also some problems to be solved before implementing this local SHM technique into real structures. Temperature dependency of PZT materials makes difficult to distinguish damage-induced variation in impedance signatures (Park *et al*. 1999). Also, a large number of PZT sensors are required in practical use since the sensing area of a single PZT sensor is very small. This local monitoring can not characterize the entire structure, which means it does not cover the entire structure but the oriented local area. That is why the activity requires locally denser sensor arrays than the global SHM.

As a new approach, a hybrid SHM methodology has been proposed to be a successful complement for both global and local SHM techniques (Hong *et al*. 2009, Kim *et al*. 2010). In the previous studies, the hybrid monitoring was based on a sequential acceleration-impedance approach, in which vibration-based global monitoring is followed by impedance-based local monitoring. However, its feasibility is restricted to damage types of quite large severities, which are enough to be detected by changes in vibration features, since local damage monitoring would not be performed as long as global monitoring is failed.

In order to overcome the limitation, a hybrid SHM scheme using a parallel acceleration-impedance approach is proposed to detect girder damage and support damage in steel plate-girder bridges which are under ambient train-induced excitations. The hybrid SHM scheme consists of three phases: global and local damage monitoring in parallel manner, damage occurrence alarming and local damage identification, and detailed damage estimation. In the first phase, damage occurrence in a structure is globally monitored by changes in vibration features and, at the same moment, damage occurrence in local critical members is monitored by changes in impedance features. In the second phase, the occurrence of damage is alarmed and the type of damage is locally identified as either girder damage or support damage by recognizing patterns of vibration and impedance features. In the final phase, the location and severity of the locally identified damage are estimated by using modal strain energy-based damage index methods. The feasibility of the proposed scheme is evaluated on a steel plate-girder bridge model which was experimentally tested under model train-induced excitations. Acceleration responses and electro-mechanical impedance signatures were measured for several damage scenarios of girder cracks and support failures.

2. Hybrid SHM for steel plate-girder bridge

2.1 Design of hybrid SHM scheme

A hybrid SHM is defined as a combined activity of global and local SHM techniques, which are classified on the basis of the acquired signal type and the inspection area (Kim *et al*. 2010). In this study, we propose a modified hybrid SHM scheme in which global SHM and local SHM are performed in parallel manner. The basic idea is that acceleration-based global SHM is carried out to globally monitor the occurrence of damage in entire structure level and, at the same time, impedance-based local SHM is carried out to pin-point damage occurrence in specified local members. This global SHM activity includes detecting damage and estimating structural safety by monitoring dynamic responses of the entire structure. Usually, vibration-based methods can estimate structural damage by utilizing the modal information obtained from limited sensor arrays; however, these methods cannot detect small incipient damage, but only detect particular forms of damage depending on sensor lay-out. Also, they need well-established baseline models to identify the perturbation from the monitored information. Contrarily, impedance-based health monitoring is the local SHM activity to acquire the information on the oriented local area, but not cover the entire structure. The basic idea is that the change in the structural integrity at a local area results in the change in electro-mechanical impedance, then damage is detected by measuring the change in impedance signatures at the local zone. This local SHM activity requires locally denser sensor arrays than the global health monitoring, so that it has the capability of detecting small incipient damage.

In this study, our concerns on the damage types are limited as girder cracks and support failures in steel plate-girder bridges. Therefore, the hybrid SHM scheme should be applicable for two damage-types of interest. In order to deal with mixed damaging scenarios, there are at least two issues: 1) how to identify damage-occurrence patterns of a unique damage-type and 2) how to custom-make health monitoring techniques for the damage-type. For each damage-type, a correct warning of damage occurrence by discriminating out of mixed information on multiple damage-types is prerequisite for damage localization and severity estimation tasks. It is also needed to

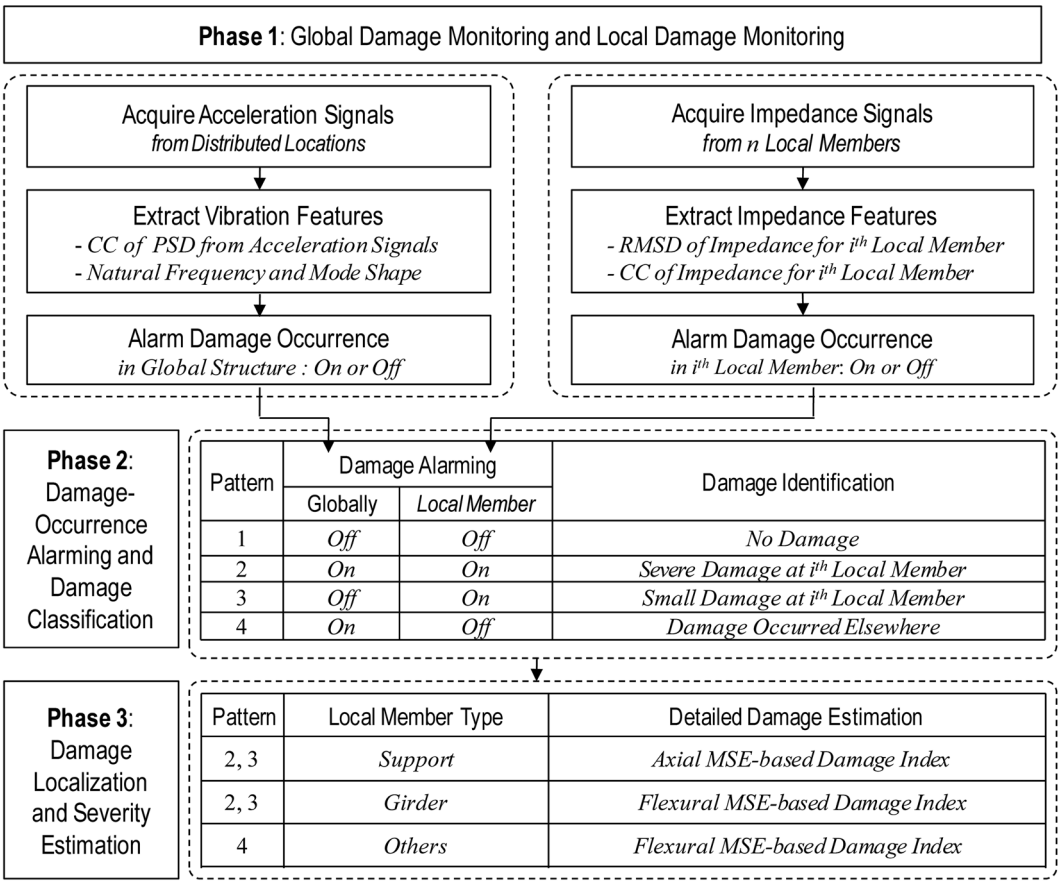

Fig. 1 Hybrid health monitoring scheme for steel plate-girder bridge

differentiate damage estimation methods suitable for each damage-type, by quantifying the variability on vibration and impedance features attributed to the two different damage-types.

To deal with those issues, a hybrid SHM scheme is designed as schematized in Fig. 1. It consists of three phases: 1) global damage monitoring in overall structure and local damage monitoring in critical sub-structural points, 2) damage-occurrence alarming and damage-type identification, and 3) damage localization and severity estimation of the identified damage.

In Phase 1, damage occurrence is globally monitored by measuring acceleration responses from the target structure. At the same moment, damage occurrence is monitored at local critical members by measuring changes in electro-mechanical impedance signatures.

Firstly, a global damage alarming method using correlation coefficient (CC) of power spectral density (PSD) and control chart analysis, as described in Section 2.2, is implemented to monitor damage occurrence in entire structure. If any damage (i.e., girder damage and support damage) occurs in the structure, the acceleration responses would be affected and consequently the CC of PSD values would be decreased.

Secondly, local damage alarming methods using impedance signatures (e.g., root-mean-square-deviation and correlation of coefficient) and control chart analysis, as described in Section 2.3, are

selected to monitor the occurrence of damage at the local sensor-vicinity zone. The impedance signatures are locally sensitive and indicative to damage occurred near a piezoelectric sensor. For example, by attaching a PZT sensor onto a support, the impedance-based local health monitoring senses mostly the change in the support but almost none of damages occurred away from the support. Also, a PZT sensor placed at the vicinity of a girder crack can monitor the change in the girder crack (e.g., crack growth); however, it is rather insensitive to any other changes occurred elsewhere. Note that the electro-mechanical impedance is sensitive to the sensor-vicinity zone but almost insensitive to the remaining structure, which makes it feasible to be indicative for the occurrence of damage in localized area.

In Phase 2, the occurrence of damage is alarmed and the type of damage is locally identified by recognizing patterns of vibration and impedance features. The alarmed damage is classified (localized) as damage occurred at specific locations (i.e., prescribed damages: girder cracks and supports) or elsewhere in the structure. There are four possible patterns of damage alarming situations: 1) No damage alerted either globally or locally, 2) Damage alerted both globally and locally, 3) Damage alerted locally but not globally, and 4) damage alerted globally but not locally. In the first pattern, no damage would be occurred in the structure if the acceleration-based monitoring does not alert damage occurrence in the entire structure and the impedance-based monitoring does not alarm damage-occurrence at the local zone. In the second pattern, damage would be apparently occurred at the local critical zone if the acceleration-based monitoring alarms the occurrence of damage in the structure and the impedance-based monitoring also alarms the occurrence of damage at the local zone. For example, the occurrence of a girder crack (or a support failure) can be identified if the acceleration-based monitoring alerts damage occurrence globally and, at the same time, the impedance-based monitoring alert damage occurrence at the pre-selected critical location. In the third pattern, incipient small damage would be occurred at a local critical zone if the acceleration-based monitoring does not alert damage occurrence but the impedance-based monitoring indicates damage occurrence at the local zone. In the final pattern, damage might be occurred elsewhere than the pre-selected local zones if the acceleration-based monitoring alarms the occurrence of damage in the structure but the impedance-based monitoring does not indicate the occurrence of damage at the local zones.

In Phase 3, the location and severity of the identified damage are estimated in details, as described in Section 2.4. If the identified damage is known as girder crack, damage is estimated by change in flexural modal strain energy which is sensitive to girder's flexural stiffness. If it is known as support damage, damage is estimated by change in axial modal strain energy which is sensitive to support's axial stiffness.

2.2 Global damage alarming by correlation coefficient of power spectral density

Damage causes the change in structural parameters (i.e., mass, damping, and stiffness), which, in turn, results in the change in vibration responses of a structure. Damage occurrence may be detected by using the change in power spectral densities of acceleration response signals. Power spectral density (PSD) may contain less noise than ordinary fast Fourier transform (FFT) results (e.g., frequency response function) since it is computed from the average of FFT results.

Assume that two acceleration signals $x(t)$ and $y(x)$ are measured before and after a damaging episode, respectively. Their corresponding power spectral densities (or auto-spectral densities) S_{xx} and S_{yy} are calculated from Welch's procedure as (Bendat and Piersol 2003)

$$S_{xx}(f) = \frac{1}{n_d T}\sum_{i=1}^{n_d}\left|X_i(f,T)\right|^2 \tag{1}$$

$$S_{yy}(f) = \frac{1}{n_d T}\sum_{i=1}^{n_d}\left|Y_i(f,T)\right|^2 \tag{2}$$

where X_i and Y_i are dynamic responses transformed into frequency domain by the discrete Fourier transform; n_d is the number of divided segments in time history; and T is data length of a divided segment.

In this study, a method using correlation coefficient (CC) of PSDs is proposed as an indicator for damage occurrence. The CC of PSDs represents the linear identity between the two PSDs obtained before and after the occurrence of damage.

$$\rho_{S_{xx}S_{yy}} = \frac{E\lfloor S_{xx}(f)S_{yy}(f)\rfloor - E\lfloor S_{xx}(f)\rfloor E\lfloor S_{yy}(f)\rfloor}{\sigma_{Sxx}\sigma_{Syy}} \tag{3}$$

where $E[\bullet]$ is the expectation operator, and σ_{Sxx} and σ_{Syy} are the standard deviations of PSDs of acceleration signals measured before and after damaging episode, respectively. If any damage occurs in the target structure, its acceleration responses would be affected and, consequently, the CCs of PSDs would be decreased. In other words, the indication by the CCs of PSDs can be a warning sign of the presence of damage (e.g., girder crack and/or support failure).

A control chart analysis is used to discriminate damage events from the CC values of PSDs (Sohn *et al*. 2001). The lower control limit (LCL) is determined as

$$LCL_\rho = \mu_\rho - 3\sigma_\rho \tag{4}$$

where μ_ρ and σ_ρ are the mean and the standard deviation of the CC values , respectively. The occurrence of damage is indicated when the CC values are beyond (i.e., less than) the bound of the LCL (Confidence level has 99.74% by range in three standard distribution); otherwise, there is no indication of damage occurrence. The control chart analysis (LCL) has basic assumption on the normal distribution.

2.3 Local damage alarming by change in electro-mechanical impedance signature

Impedance-based SHM techniques utilize piezoelectric sensors such as PZT or MFC patches which are locally sensitive to its sensor-vicinity area. As shown in Fig. 2, the piezoelectric material is described by its short circuited mechanical impedance, which is powered by voltage or current (Liang *et al*. 1996). The host structure is modeled as the effect of mass, stiffness, damping, and boundary conditions. The electrical impedance of the piezoelectric patch bonded onto a host structure is directly related to the mechanical impedance of the structure. When damage occurs to a structure, its mechanical impedance would be changed. Hence, any changes (such as magnitude of admittance and resonant frequency) in the electrical impedance signature are attributed to damage or changes in mechanical property of the local sensor-vicinity zone (Giurgiutiu and Zagrai 2002, Bhalla and Soh 2004, Park *et al*. 2005, Park *et al*. 2006).

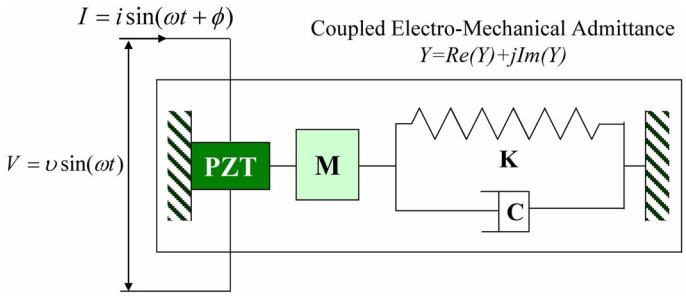

Fig. 2 1-D Model of electro-mechanical interaction of piezoelectric patch and host structure (Liang *et al.* 1996)

2.3.1 Root Mean Square Deviation (RMSD) of impedance signatures

To quantify the change in impedance signature due to damage in the structure, the root-mean-square-deviation (RMSD) of impedance signatures measured before and after damage (Sun *et al.* 1995) is used in this study. The RMSD is calculated from impedance measurements before and after damage as

$$RMSD(Z, Z^*) = \sqrt{\sum_{i=1}^{N}[Z^*(\omega_i) - Z(\omega_i)]^2 / \sum_{i=1}^{N}[Z(\omega_i)]^2} \tag{5}$$

where $Z(\omega_i)$ and $Z^*(\omega_i)$ are impedances measured before and after damage for i^{th} frequency, respectively; and N denotes the number of frequency points in the sweep. The RMSD equals to 0 if no damage. Otherwise, the RMSD is larger than 0.

Due to experimental and environmental errors, however, the RMSD may be larger than 0 although damage is not occurred. To deal with the uncertain conditions, the control chart analysis is used for decision-making out of the RMSD values. In this study, the upper control limit (UCL) is adopted for alarming damage occurrence, as follows

$$UCL_{RMSD} = \mu_{RMSD} + 3\,\sigma_{RMSD} \tag{6}$$

where μ_{RMSD} and σ_{RMSD} are mean and standard deviation of RMSDs, respectively. The occurrence of damage is indicated when the RMSD values are beyond (i.e., larger than) the bound of the UCL (Confidence level has 99.74% by range in three standard distribution). Otherwise, there is no indication of damage occurrence. The control chart analysis (UCL) has basic assumption on the normal distribution.

2.3.2 Correlation coefficient of impedance signatures

Similar to the previous description, correlation coefficient of impedance signatures between before and after damage is computed as follows (Koo 2008)

$$\rho_{Z,Z^*} = \frac{E\lfloor Z(\omega)Z^*(\omega)\rfloor - \mu_Z\,\mu_{Z^*}}{\sigma_Z \sigma_{Z^*}} \tag{7}$$

where $Z(\omega)$ and $Z^*(\omega)$ are impedance signatures of a frequency band measured before and after

damage, respectively. Also, μ_Z and σ_Z are mean and standard deviation values of impedance signals. Control chart analysis is used to alert damage occurrence from the correlation coefficients of impedance signatures. Lower control limit is determined similarly as described in Eq. (4).

2.4 Damage estimation by modal strain energy-based damage index method

2.4.1 Damage localization

Based on the earlier formulation proposed by Kim and Stubbs (1995, 2002) proposed an improved damage index method using changes in modal strain energies. Modal strain energy (MSE) is a damage sensitive feature using mode shape curvature. The MSE-based damage index method is based on the decrease in MSE between two structural systems. Damage in the j^{th} member is defined as the relative change between undamaged stiffness, k_j, and damaged one, k_j^*, of the same element. For all available NM vibration modes, the MSE-based damage index for the j^{th} location, β_j, is given by (Kim and Stubbs 2002)

$$\beta_j = \frac{k_j}{k_j^*} = \sum_{i=1}^{M} \gamma_{ji}^* / \sum_{i=1}^{M} (\gamma_i g_i + \gamma_{ji}) \tag{8}$$

where γ_i represents the i^{th} modal stiffness and γ_{ji} represents the contribution of the j^{th} element to the i^{th} modal stiffness. Both γ_i and γ_{ji} are free from material and geometric quantities. The term g_i is a dimensionless factor representing the fractional changes in the i^{th} modal parameters (i.e., $g_i = \delta\omega_i^2/\omega_i^2$). Note the stiffness is assumed as constant over the j^{th} member of the structure (i.e., $k_j = k(\hat{x}) = \text{constant}$). Note also the asterisk denotes damaged state.

Noticing that girder and support are two primary targets of damage detection, the MSE-based damage index of Eq. (8) should be adapted to meet the two separate structural models: flexural beam for girder and axial rod for support. Accordingly, girder damage will be estimated as the fractional change in flexural stiffness. Similarly, the support damage will be estimated as the fractional change in axial stiffness.

First, girder is modeled as Euler-Bernoulli beam from which damage is defined as the change in flexural stiffness. To represent flexural modal strain energies and to estimate girder damage accordingly, γ_i, γ_{ji} and γ_{ji}^* are formulated as follows (Kim and Stubbs 2002): $\gamma_{ji} = \int_j [\phi_i''(x)]^2 dx$, $\gamma_{ji}^* = \int_j [\phi_i''^*(x)]^2 dx$, and $\gamma_i = \int_0^L [\phi_i''(x)]^2 dx$. The term $\phi_i''(x)$ is mode shape curvature of i^{th} modal vector and it is computed from i^{th} mode shape vector $\phi_i(x)$ which is measured vertically from the girder.

Next, support is modeled as axially deformable rod from which damage is defined as the change in axial stiffness. To estimate support damage by using changes in axial modal strain energies, γ_i, γ_{ji} and γ_{ji}^* are formulated as follows: $\gamma_{ji} = \int_j [\phi_i(x)]^2 dx$, $\gamma_{ji}^* = \int_j [\phi_i^*(x)]^2 dx$, and $\gamma_i = \int_0^L [\phi_i(x)]^2 dx$. The i^{th} mode shape vector $\phi_i(x)$ is measured vertically (axially) on the supports. In this subsystem, the number of elements is the same as the number of supports.

For damage localization practice, the damage indices (i.e., Eq. (8)) are normalized according to the standard rule as

$$Z_j = (\beta_j - \mu_\beta)/\sigma_\beta \tag{9}$$

where μ_β and σ_β represent, respectively, the mean and standard deviation of the collection of β_j values. Then, the damage is localized from the statistical hypothesis tests. The null hypothesis (i.e., H_o) is taken to be the structure undamaged at j^{th} element and the alternate hypothesis (i.e., H_1) is taken to be the structure damaged at j^{th} element. In assigning damage to a particular location, the following decision rule is utilized: 1) choose H_1 if $Z_j \geq z_o$; and 2) choose H_o if $Z_j < z_o$, where z_o is number which depends upon the confidence level of the localization test. Then damage is assigned to a particular location j if Z_j exceeds the confidence level.

2.4.2 Damage severity estimation

Once damage is located at the j^{th} location, the severity of damage is estimated at the same element directly from Eq. (8). The severity estimation index for the j^{th} element, α_j, is given by (Kim and Stubbs 2002)

$$\alpha_j = \frac{k_j^* - k_j}{k_j} = \left[\sum_{i=1}^{M} (\gamma_{ji} - \gamma_{ji}^*) + \sum_{i=1}^{M} \gamma_i \, g_i\right] \Big/ \sum_{i=1}^{M} \gamma_{ji}^* \tag{10}$$

where the damage severity is defined as the fractional change in stiffness of the j^{th} element. For a girder element which is represented by flexural stiffness, the severity of damage will be estimated by using the change in flexural modal strain energy, as described previously. For a support element which is represented by the change in axial modal strain energy, the severity estimation index for the k^{th} support, as described previously.

3. Experiment on steel plate-girder bridge model

3.1 Test structure and experimental setup

The test structure is a single-span, stainless steel, plate-girder bridge model, as shown in Fig. 3. Its superstructure consists of deck, girders, stiffeners, floor beams, stringers, and piers. The bridge spans 2.0-m and is simply supported with pin-pin conditions. The girders are supported by bearing plates and piers. A bearing plate and a pier are connected by four bolts. Each pier consists of a steel column and four steel rods to stabilize the column by piling onto a steel block. In total, four steel blocks and a system of steel frame bases are utilized to setup the test structure.

Locations and arrangements of sensors on the test structure were designed as shown in Figs. 3 and 4. For acceleration measurement, fourteen accelerometers were installed on the deck of the model bridge. Seven accelerometers were placed along each girder with constant interval: Acc 1 – Acc 7 on Girder 1 and Acc 8 – Acc 14 on Girder 2. Note that a sensor was located at a girder edge which is on top of a support (e.g., Acc 1 on Support A). A type of ICP accelerometers were used in the test: PCB 393B04 with a nominal sensitivity of 1V/g and a specified frequency range ($\pm 3dB$) of 0.02~1.7 kHz. The data acquisition system included a 16-channels PCB Signal Conditioner, Terminal Block and MATLAB.

Ambient excitation was applied by a model train passing between two girders on the bridge

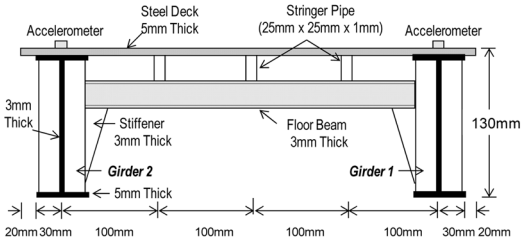

(a) Cross-Section

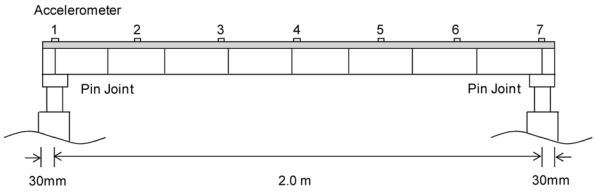

(b) Plane View

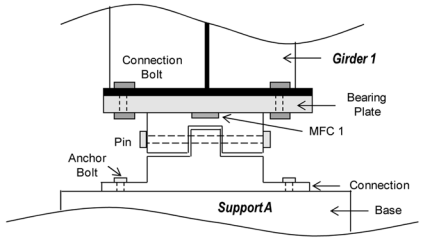

(c) Support System

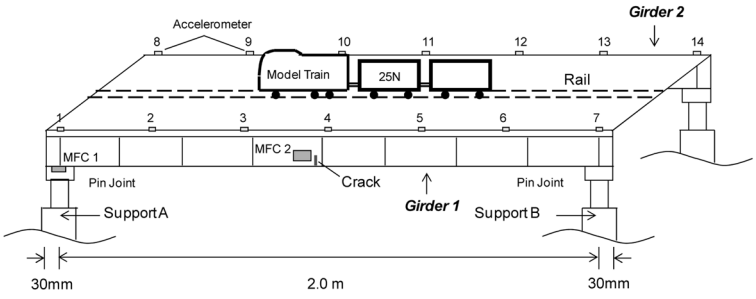

(d) Test Setup

Fig. 3 Schematic of plate-girder bridge model

model. The controllable train speed was maximum speed of about 0.48 m/s by electric train model. By considering lab-scaled bridge model was scaled down about 1/25-1/30, that the train speed equivalent to about 40-50 km/hr speed in real structures. The model train was carrying about 25*N* weight (including its self-weight) and it caused relatively low acceleration level. Then dynamic responses in vertical direction were measured from the fourteen sensors, Acc 1 – Acc 14, with a

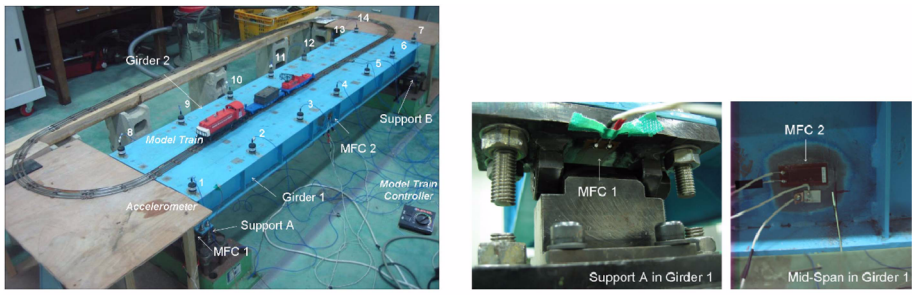

(a) Model Train and Accelerometers (b) MFC Sensors

Fig. 4 Experimental setup in plate-girder bridge model

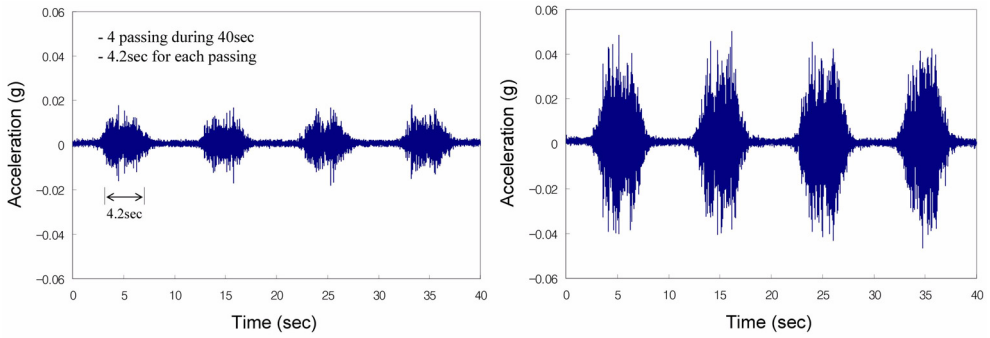

(a) Acc 1 (b) Acc 3

Fig. 5 Acceleration response signals from two accelerometers

sampling frequency of 500 Hz. Fig. 5 shows two acceleration response signals measured from two sensors (Acc 1 and Acc 3) for 40 seconds during four cycles of train passing on the model bridge. It is noticed that Acc 1 locates on top of Support A and is the last sensor to start measuring response signals as the train enters the bridge from Support B.

Modal parameters were extracted from the acceleration response signals by using frequency-domain decomposition (FDD) method which is an output-only modal analysis technique (Brincker *et al*. 2001, Yi and Yun 2004). Fig. 6 shows two power spectral densities corresponding to of the two acceleration signals shown in Fig. 5. For the calculation of PSDs, the cut-off frequency was set to 250 Hz, and acceleration signals were overlapped 90% to reduce effect of random noises. Figure 7 shows mode shapes and natural frequencies of the first two modes (i.e., 1st bending and 1st torsion modes) measured from the fourteen sensors for the undamaged reference state.

For impedance measurement, two impedance sensors were installed on the test bridge, as shown in Figs. 3 and 4. A type of piezo-ceramic fiber composite sensor was used: Macro-Fiber Composite (MFC) with a size of 25.4 × 12.7 × 0.254 mm and the Young's modulus is 15 GPa. The MFC patch is more flexible and less affected by bonding defects than ordinary PZT patches. We selected two critical locations for the two impedance sensors, i.e., monitoring support damage (i.e., change in

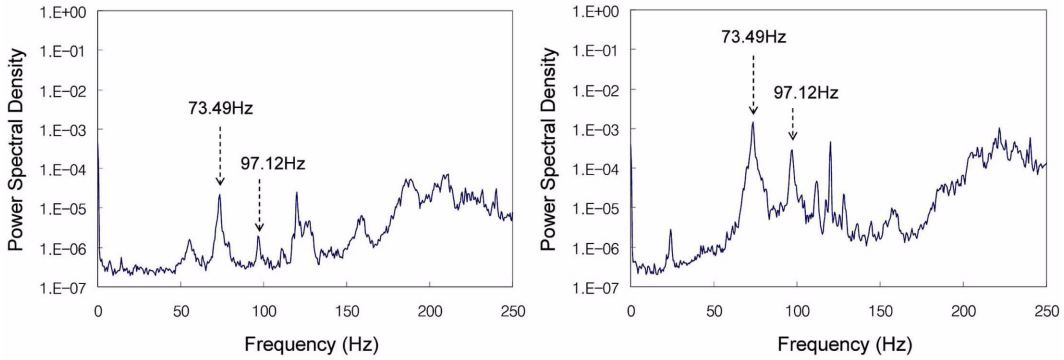

(a) PSD from Acc 1 (b) PSD from Acc 3

Fig. 6 Power spectral densities (PSDs) extracted from acceleration signals

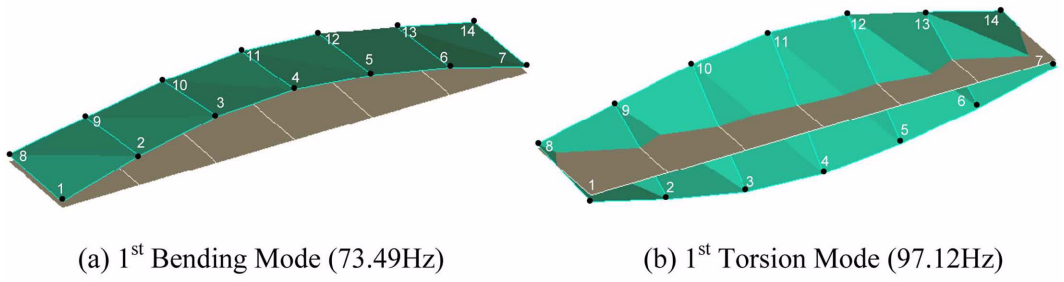

(a) 1st Bending Mode (73.49Hz) (b) 1st Torsion Mode (97.12Hz)

Fig. 7 Mode shapes and natural frequencies for undamaged structure

local support conditions) and girder damage (i.e., change in local girder-section properties). As the first impedance sensor, a MFC patch (MFC 1) was bonded to directly monitor support damage on the bottom surface of the bearing plate of Support A. As the second impedance sensor, another MFC patch (MFC 2) was bonded to directly monitor girder damage on the web surface near the mid-span of Girder 1 where a pre-cut existed.

The data acquisition system included an impedance analyzer HIOKI 3532 and a PC with LabVIEW software. The input voltage into the MFC patches was set up as 1 V. The system was set up to measure self-diagnosis signals from the MFC sensors and furthermore to extract real parts of impedance signatures. Fig. 8 shows two impedance signatures measured from MFC 1 sensor at Support A and MFC 2 sensor at the mid-span of Girder 1, respectively, for the undamaged reference state.

A series of tests to measure acceleration responses and impedance responses were performed in a lab on 17 August, 2009. The lab was air-conditioned to keep temperature and humidity close to constant during the tests. As shown in Fig. 9, air temperatures ranged from 23.42°C to 24.14°C. There were very slight changes in air temperatures near the test bridge; therefore, the effect of temperature changes on the experiments is not accounted in this study.

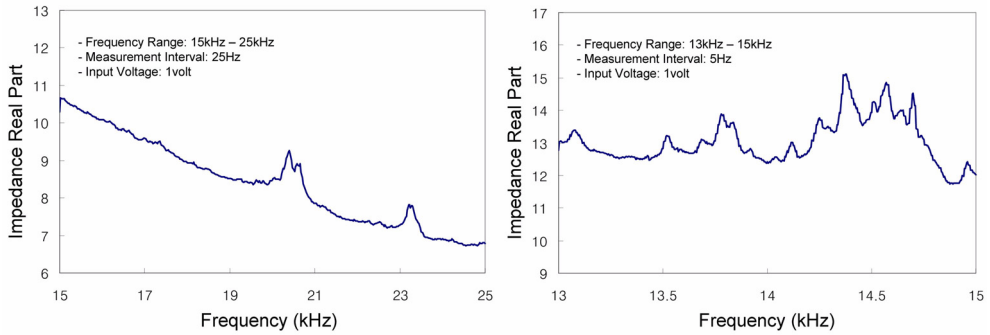

(a) MFC 1 (b) MFC 2

Fig. 8 Impedance signatures from two impedance sensors

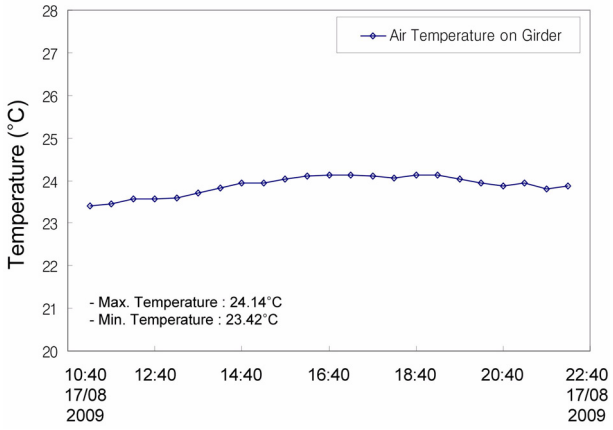

Fig. 9 Air temperature records during experiment

3.2 Evaluation of global and local monitoring methods

3.2.1 Global damage monitoring method

The feasibility of the global monitoring method is evaluated for the plate-girder bridge model. The performance of the CC of PSDs (Eq. (3)) is compared with that of frequency change. For the evaluation, two different damage types of interest (i.e., girder damage and support damage) were simulated in the test structure and acceleration responses were measured from two accelerometers (Acc 1 and Acc 3) in the test structure. As shown in Fig. 10, a girder damage case *Girder 1_Crack* was simulated by a 30 mm cut of girder-web at mid-span nearby Acc 4 on Girder 1. Also, a support damage case *Support A_3Bolts* was simulated by loosening three connection bolts (Bolt 1-Bolt3) at Support A.

As shown in Fig. 11, natural frequencies change to alert the occurrence of the girder damage, *Girder 1_Crack*; however, they do not change sensitively enough to alert the occurrence of the support damage, *Support A_3Bolts*. As shown in Fig. 12, the PSDs (of both Acc 1 and Acc 3) change as damage occurs. The CCs of PSDs correctly indicate the occurrence of the support

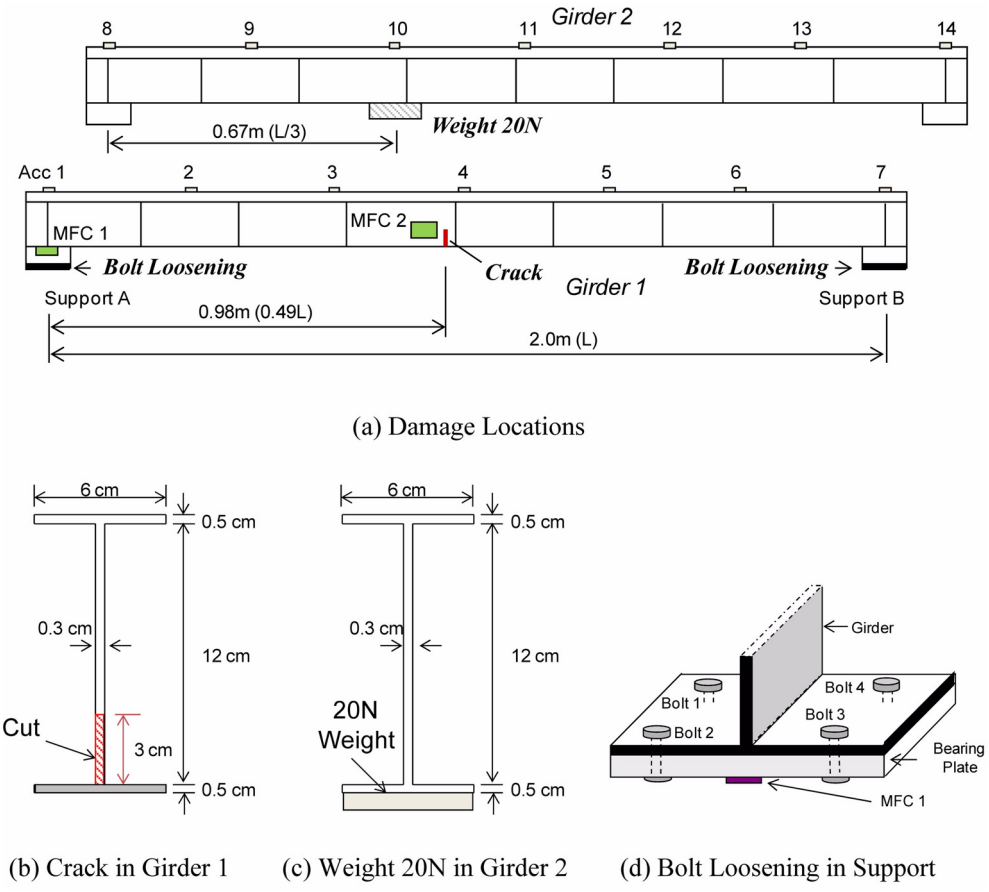

Fig. 10 Schematic of simulated damage in test structure

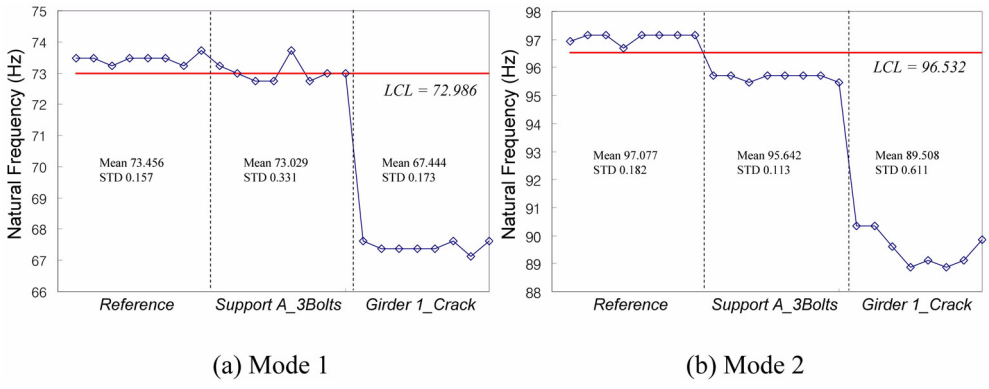

Fig. 11 Frequency change for two damage cases in test structure

damage (*Support A_3Bolts*) as well as the girder damage (*Girder 1_Crack*). Also, it is noticed that the CCs of PSDs from Acc 3 are more sensitive to damage than Acc 1 results.

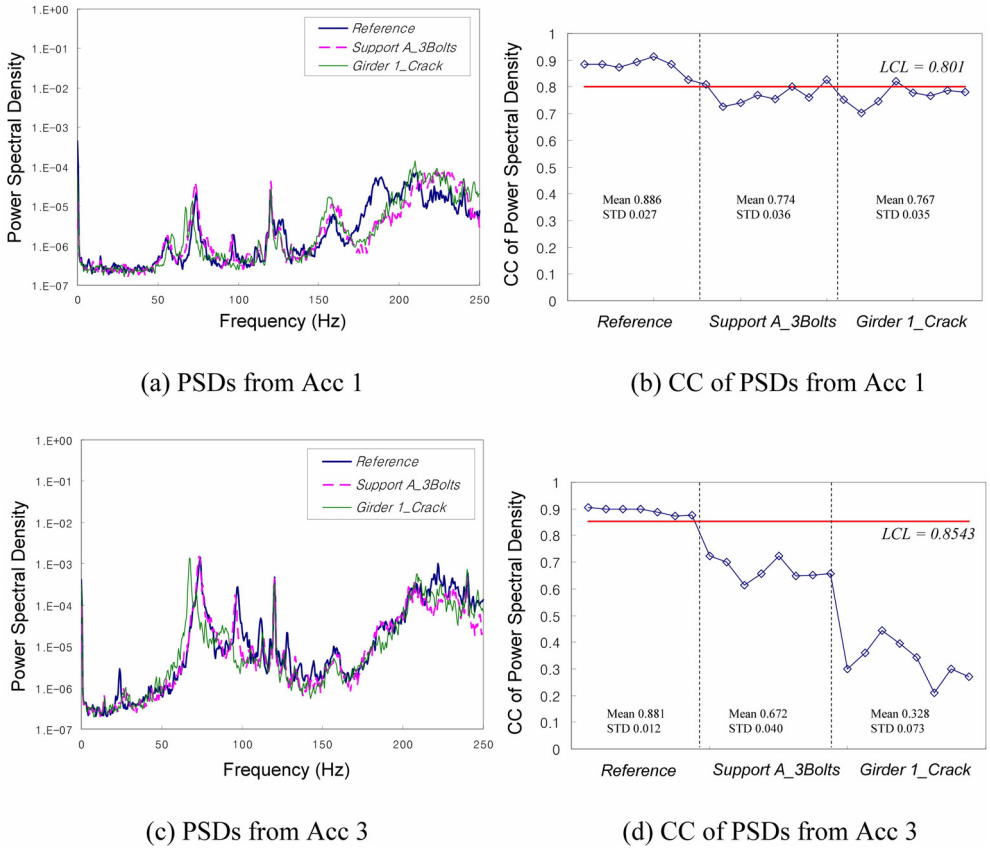

(a) PSDs from Acc 1 (b) CC of PSDs from Acc 1

(c) PSDs from Acc 3 (d) CC of PSDs from Acc 3

Fig. 12 CC of PSDs for girder and support damage cases in test structure

3.2.2 Local damage monitoring method

The feasibility of the local monitoring methods is evaluated for the test structure. The performance of the RMSD of impedance signatures (Eq. (5)) is compared with that of the CC of impedance signatures (Eq. (7)). For the evaluation, two girder damages and two support damages were simulated in the test structure and impedance signatures were measured from the two impedance sensors (MFC 1 and MFC 2) which are described in Fig. 3. As shown in Fig. 10, two girder damages are simulated as: (1) *Girder 1_Crack* - a 30mm cut of girder-web at mid-span nearby Acc 4 on Girder 1 and (2) *Girder 2_Weight* - a 20N weight load at 1/3 span length nearby Acc 10 on Girder 2. Also, two support damages are simulated as: (1) *Support A_3Bolts* - loosening three connection-bolts at Support A and (2) *Support B_3Bolts* - loosening the three connection bolts (Bolt 1-Bolt 3) at Support B. The initial torque for four connection bolts (Bolt 1-Bolt 4) at Supports A and B were applied by checking with hand sense.

As shown in Fig. 13, impedance signatures were monitored from MFC 1 and MFC 2 sensors and then the RMSDs of impedance signatures were computed for the four damage cases. As also shown in Fig. 14, the CCs of impedance signatures were monitored for the four damage cases. From Figs. 13 and 14, it is observed that MFC 1 (which locates at Support A) accurately indicated the occurrence of damage at Support A (*Support A_3Bolts*). Meanwhile, MFC 2 (which locates at the

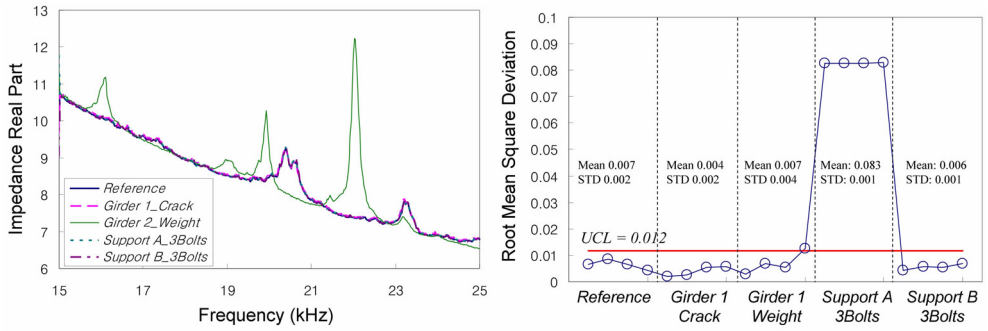

(a) Impedance Signatures from MFC 1 (b) RMSD Changes from MFC 1

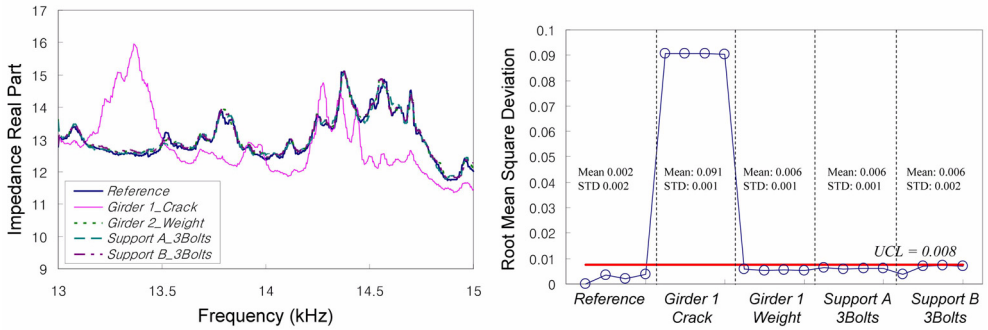

(c) Impedance Signatures from MFC 2 (d) RMSD Changes from MFC 2

Fig. 13 RMSD of impedance signals for four damage cases in test structure

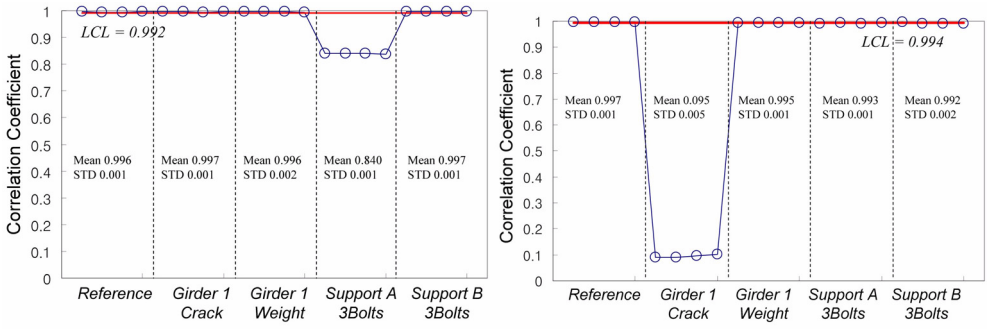

(a) CC Changes from MFC 1 (b) CC Changes from MFC 2

Fig. 14 CC of impedance signatures for four damage cases in test structure

vicinity of the mid-span of Girder 1) accurately indicated the occurrence of damage at the mid-span of Girder 1 (*Girder 1_Crack*). Both MFC 1 and MFC 2 were sensitive to their vicinity-damages nearby their local points. However, they were insensitive to other damages away from them. For

example, MFC 2 alarms the girder crack in its 3cm vicinity (*Girder 1_Crack*) but it does not alert the weight-load in 80cm distance, (*Girder 2_Weight*), or the support changes in 100cm distance (*Support A_3Bolts* and *Support B_3Bolts*). It is also noticed from Figs. 13 and 14 that the overall performance of the RMSDs is relatively better than the CCs.

4. Hybrid SHM in plate-girder bridge model

4.1 Hybrid SHM for girder damage

As described in Fig. 10, a girder crack (*Girder 1_Crack*) was introduced into the girder by inflicting a 30mm cut of girder-web at mid-span nearby Acc 4 on Girder 1. Damage monitoring was performed in the following three phases.

4.1.1 Phase 1 - global damage monitoring and local damage monitoring

Firstly, the occurrence of damage was monitored in a global manner by using the CC of PSDs of Eq. (3). For each of undamaged and damaged states, acceleration signals were measured up to eight ensembles from Acc 3. For each ensemble, acceleration responses were recorded for 40 seconds during four cycles of train passing on the model bridge. As shown in Fig. 15, the CCs of PSDs were obtained for the undamaged reference state and also for the girder damage case. Eight ensembles of the undamaged state were used to decide the LCL value of 0.854 by using Eq. (4). The CC value beyond the LCL criteria indicates the occurrence of damage in the bridge model, as shown in Fig. 15.

Secondly, the occurrence of damage was monitored from MFC 1 and MFC 2 impedance sensors at two local critical points, as shown in Figs. 3 and 4. The RMSDs of impedance signatures were calculated by Eq. (6). As shown in Fig. 16, the RMSDs for MFC 2 (which locates at the vicinity of the mid-span of Girder 1) increase beyond the bound of UCL but not in MFC 1 (which locates at Support A) as the girder damage occurred at the vicinity of the mid-span of Girder 1.

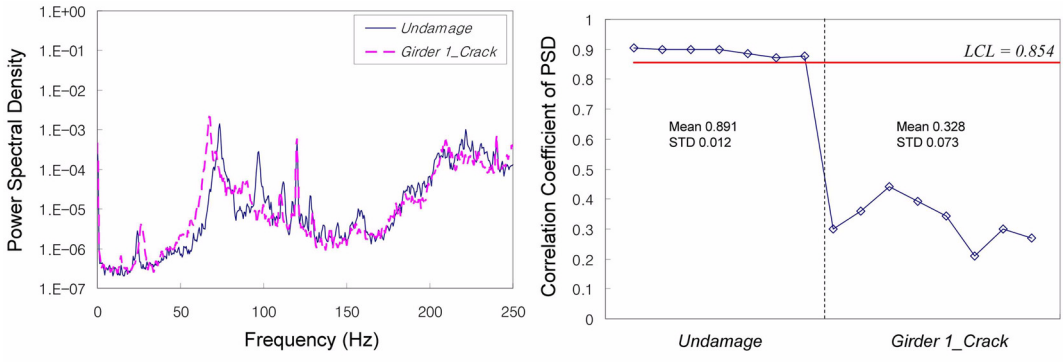

(a) PSD of Acc 3 (b) CC of PSD of Acc 3

Fig. 15 CC of PSDs for girder damage in test structure

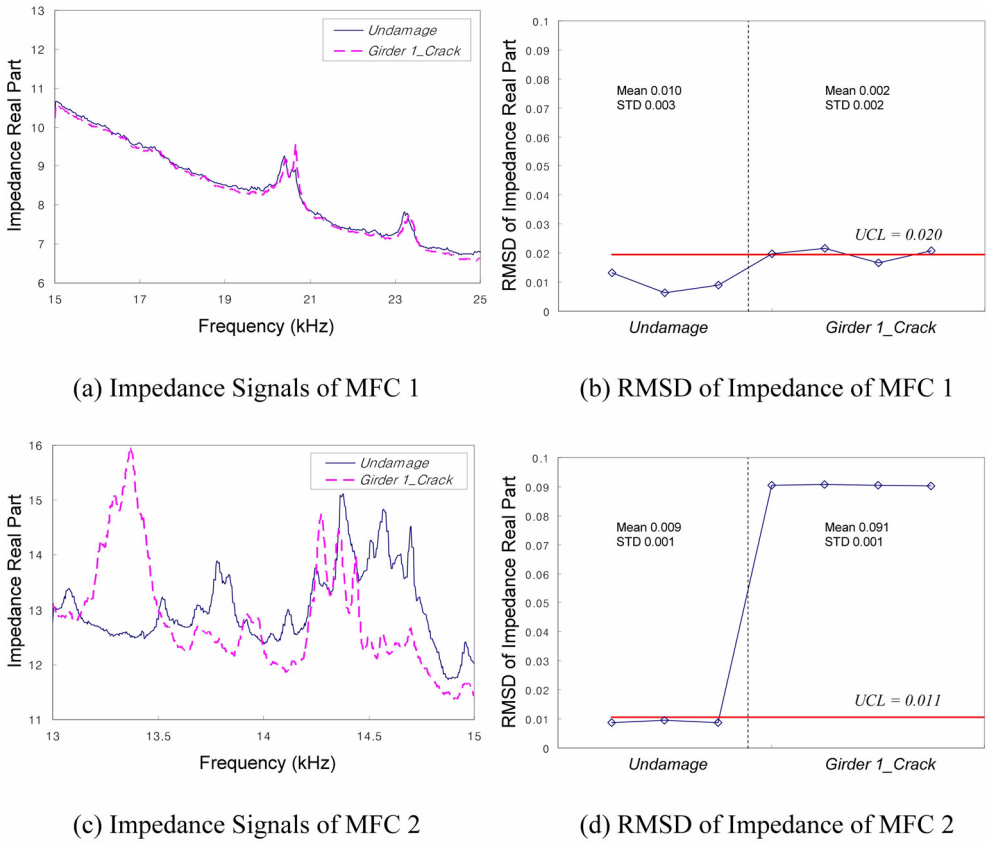

(a) Impedance Signals of MFC 1 (b) RMSD of Impedance of MFC 1

(c) Impedance Signals of MFC 2 (d) RMSD of Impedance of MFC 2

Fig. 16 RMSD of impedance signatures for girder damage in test structure

Table 1 Damage-type identification in test structure: girder damage

Damage Case	Global Alarming by CC of PSDs (Acc 3)	Local Alarming by RMSD of Impedance		Damage-Type Identification
		MFC 1 At Support A	MFC 2 At L/2 of Girder 1	
Girder1_Crack	O	–	O	Damage at L/2 of Girder 1

4.1.2. Phase 2 - damage-occurrence alarming and damage classification

In Phase 2, damage occurrence is alarmed and damage type is classified. As outlined in Table 1, global alarming is indicated in Acc 3 sensor by the CC of PSDs, which means the occurrence of damage in the global structure. Also, local alarming is indicated in MFC 2 sensor by the RMSD of impedance signatures, which means the occurrence of damage in the local zone. These results indicate that the alerted damage is identical to Pattern 2 of Phase 2 in Fig. 2 and identified as girder damage near the mid-span of Girder 1.

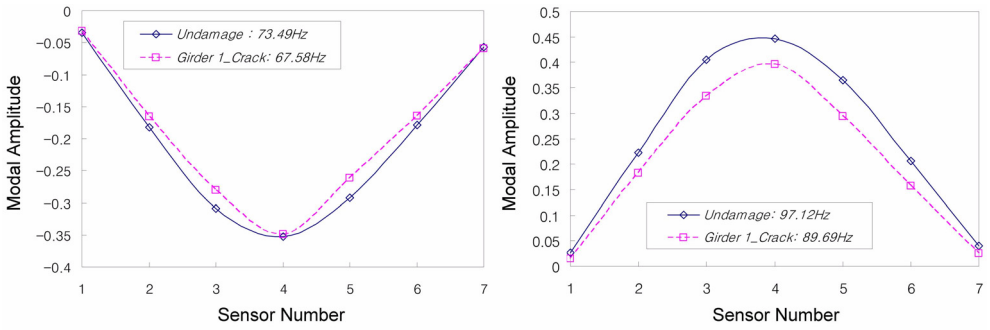

(a) Mode 1: 1st Bending (b) Mode 2: 1st Twist

Fig. 17 Mode shapes of girder 1 of test structure: undamaged and girder damage cases

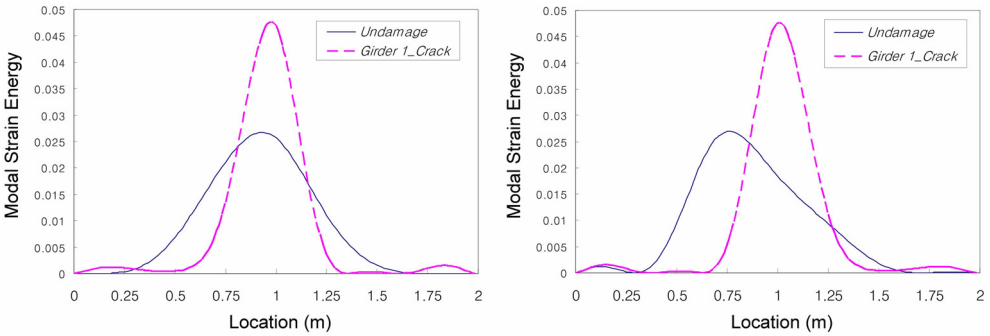

(a) Mode 1: 1st Bending (b) Mode 2: 1st Twist

Fig. 18 Modal strain energies of girder 1 of test structure: undamaged and girder damage cases

4.1.3 Phase 3 - damage localization and severity estimation

In Phase 3, the identified damage was estimated in detail. Since the alerted damage was classified as girder damage near the mid-span of Girder 1, the MSE-based damage index method was utilized to locate and estimate the severity of damage in the girder. For the girder damage case, natural frequencies and mode shapes of the first two modes were extracted from acceleration signals measured at the seven sensors, Acc 1- Acc 7. Fig. 17 shows the first two mode shapes of Girder 1 and the corresponding natural frequencies measured for the undamaged reference and the girder damage case.

The damage location index, β_j, was computed according to Eq. (8). As shown in Fig. 18, flexural modal strain energies of girder elements were computed from modal curvatures which were analyzed from mode shapes by using cubic-spline interpolation functions. As shown in Fig. 19, the normalized damage indices were computed by Eq. (9). In assigning damage to a particular location, the decision rule was utilized as: (1) Choose H_1 if $Z_j \geq 2.0$; and 2) choose H_o if $Z_j < 2.0$. The objective threshold of 2.0 was selected with a confidence level of 97.2%. By using only mode 1, as shown in Fig. 19(a), damage locations were predicted as 0.46L-0.51L. By noticing the real damage

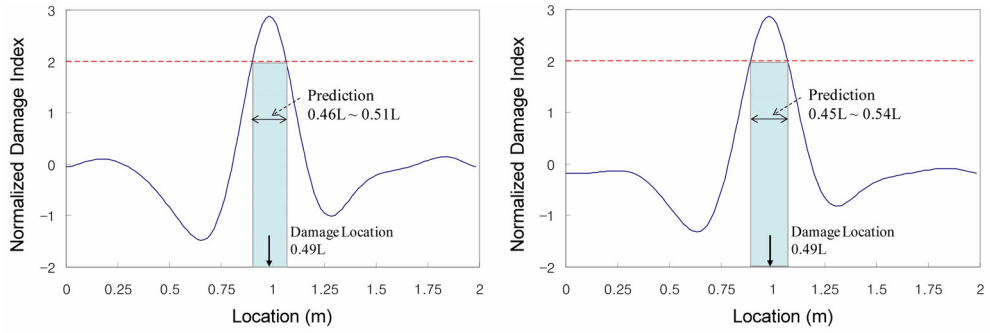

(a) Localization by Mode 1 (b) Localization by Modes 1 and 2

Fig. 19 MSE-based damage location index results for girder 1 of test structure

Table 2 Natural frequencies for three support damage cases in test structure

Damage Case	Damage Scenario	Natural Frequency (Hz)	
		Mode 1	Mode 2
Undamaged Reference	–	73.49	97.12
Support A_1Bolt	1 Bolt Loosened At Support A	73.38	97.20
Support A_2Bolts	2 Bolts Loosened At Support A	73.50	97.26
Support A_3Bolts	3 Bolts Loosened At Support A	73.07	95.64

was located at 0.49L, the prediction results were 2-3% location errors with respect to the span length. By using modes 1 and 2 together, as shown in Fig. 19(b), damage locations were predicted as 0.45L-0.54L, showing 3-5% location errors.

Once damage locations were predicted, severities of damage, α_j, were estimated by using Eq. (10). At the peak point in Fig. 19(a), the severity of damage was estimated as 79% loss of flexural stiffness ($\alpha_j = -0.79$). Note that the actual inflicted crack is equivalent to 53% stiffness-loss ($\alpha_j = -0.53$) by considering the fractional loss of flexural rigidity of the cracked section shown in Figs. 3 and 4 (here, the change in the second moment of area is only counted). It is noted that the severity was over-estimated with about 30% error.

4.2 Hybrid SHM of support damage

Three levels of support damage were inflicted to connection bolts in Support A as shown in Figs. 3 and 4. As outlined in Table 2, the damage levels were described as the number of loosened bolts. For the support damage cases (*Support A_1Bolt*, *Support A_2Bolts*, and *Support A_3Bolts*), natural frequencies measured from acceleration responses are also outlined in Table 2. Damage monitoring was performed in the following three phases.

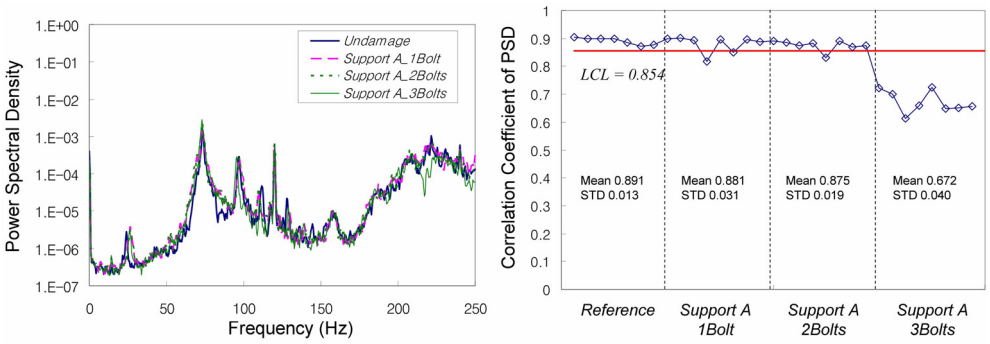

(a) PSD of Acc 3 (b) CC of PSD of Acc 3

Fig. 20 CC of PSDs for support damage cases in test structure

4.2.1 Phase 1 - global damage monitoring and local damage monitoring

Firstly, the occurrence of damage was monitored in a global manner by using the CC of PSDs of Eq. (3). For each of undamaged and damaged states, acceleration signals were measured up to eight ensembles from Acc 3. For each ensemble, acceleration responses were recorded for 40 seconds during four cycles of train passing on the model bridge. As shown in Fig. 20, the CCs of PSDs were obtained for undamaged reference state and also for three support damage cases. Eight ensembles of the undamaged state were used to decide LCL value of Eq. (4). The CC value beyond the LCL criteria indicates the occurrence of damage in the bridge model, as shown in Fig. 20. Damage occurrence was successfully alerted in *Support A_3Bolts*, but not in *Support A_1Bolt* and *Support A_2Bolts* which are relatively small damages.

Secondly, the occurrence of damage was monitored from MFC 1 and MFC 2 impedance sensors at two local critical points, as shown in Fig. 3 and Fig. 4. The RMSDs of impedance signatures were calculated by Eq. (5). As shown in Fig. 21, the RMSDs for MFC 1 (which locates at Support A) increase beyond the bound of UCL value as the support damages occur at the connection bolts of Support A. However, the RMSDs in MFC 2 sensor (which locates at the vicinity of the mid-span of Girder 1) remain almost unchanged.

4.2.2 Phase 2 - damage-occurrence alarming and damage classification

In Phase 2, damage occurrence is alarmed and damage type is classified. As outlined in Table 3, global alarming is indicated by the CC of PSDs measured at Acc 3 sensor. Also, local alarming is indicated by the RMSD of impedance signatures measured from MFC 1 sensor. For the first two damage cases (i.e., *Support A_1Bolt* and *Support A_2Bolts*), the global and local SHM results indicate the occurrence of incipient (small) damage at Support A since there was local alarming by MFC 1 (at Support A) but not global alarming by Acc 3. This result is identical to Pattern 3 in Fig. 1 (Note that there were no significant changes in the CCs of PSDs enough to alarm damage occurrence in the global structure). For *Support A_3Bolts*, the hybrid SHM results indicate the occurrence of damage at Support A. There were both global alarming by the CCs of PSDs and also local alarming at Support A by the RMSDs of impedance signatures from MFC 1. This is identical to Pattern 2 in Fig. 1.

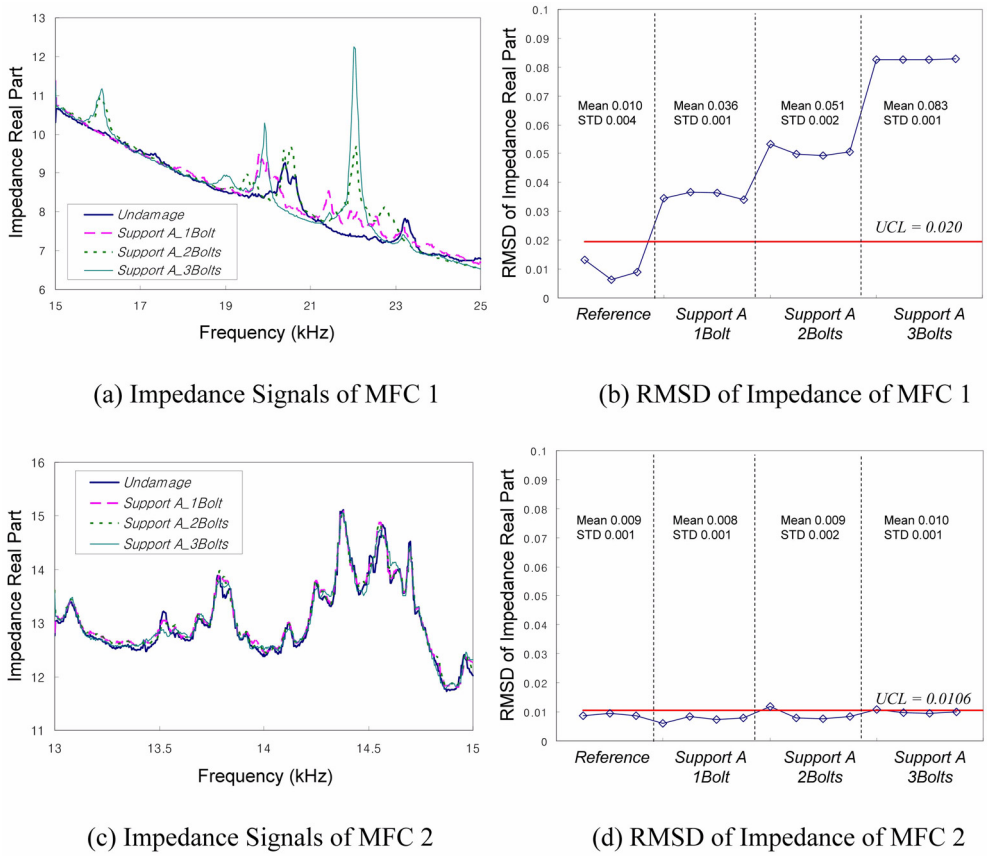

(a) Impedance Signals of MFC 1 (b) RMSD of Impedance of MFC 1

(c) Impedance Signals of MFC 2 (d) RMSD of Impedance of MFC 2

Fig. 21 RMSD of impedance signatures for support damage cases in test structure

Table 3 Damage-type identification in test structure: support damage

Damage Case	Global Alarming by CC of PSDs (Acc 3)	Local Alarming by RMSD of Impedance		Damage-Type Identification
		MFC 1 At Support A	MFC 2 At L/2 of Girder 1	
Support A_1Bolt	–	O	–	Incipient Damage At Support A
Support A_2Bolts	–	O	–	Incipient Damage At Support A
Support A_3Bolts	O	O	–	Damage At Support A

4.2.3 Phase 3 - damage localization and severity estimation

In Phase 3, the identified damage was estimated in detail. Since the alerted damage was classified as support damage at Support A, the MSE-based damage index method was utilized to locate and estimate the severity of damage in the supports. As listed in Table 4, modal values of the first two

Table 4 Modal amplitudes at support a and support b in girder 1: undamaged and 3 support damaged cases

Sensor Number (Support)	Mode 1 (1st Bending)				Mode 2 (1st Twist)			
	Undamaged Reference (73.49 Hz)	*Support A _1Bolt* (73.38 Hz)	*Support A _2Bolts* (73.50 Hz)	*Support A _3Bolts* (73.07 Hz)	Undamaged Reference (97.12 Hz)	*Support A _1Bolt* (97.20 Hz)	*Support A _2Bolts* (97.26 Hz)	*Support A _3Bolts* (95.64 Hz)
Acc 1 (Support A)	-0.0339	-0.0366	-0.0368	-0.0551	0.0273	0.0257	0.0255	0.0563
Acc 7 (Support B)	-0.0566	-0.0603	-0.0597	-0.0542	0.0398	0.0397	0.0396	0.0319

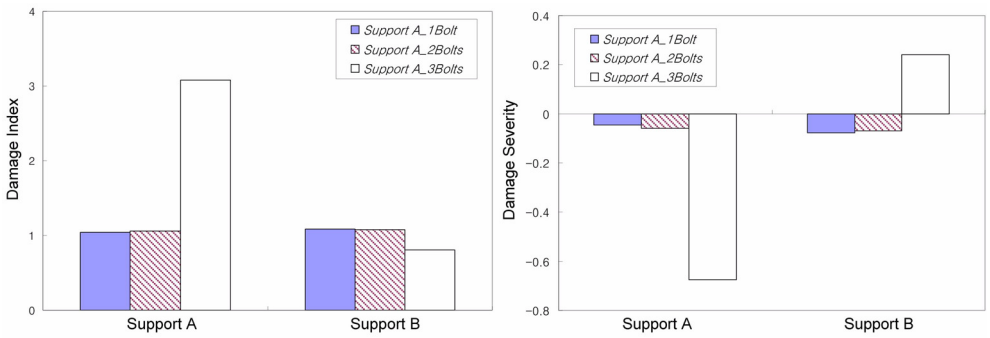

(a) Damage Location (b) Damage Severity

Fig. 22 Damage estimation results of supports in girder 1 of test structure

modes were extracted for the undamaged reference and the three support damage cases. Then axial modal strain energies of the two modes were computed of the two support elements (Support A and Support B) in Girder 1.

As shown in Fig. 22(a), the damage location index, β_j, was computed according to Eq. (8) by using modes 1 and 2 together. As shown in Fig. 22 (b), severities of damage, α_j, were estimated by using Eq. (10). Both figures indicate that the noticeable damage localization is predicted for only Support Damage 3. For the indication, damage was located correctly at Support A and also its severity was estimated as of 69% loss of axial stiffness (i.e., $\alpha_j = -0.68$ in Fig. 22(b)). It is noted for Support Damage 3 that the actual inflicted severity was 3 bolts loosened out of 4 bolts at the support connection and it corresponds to about 75% loss of total axial stiffness. For Support Damage 1 and Support Damage 2, damage severities were estimated as of 4-5% loss of axial stiffness at Support A.

5. Conclusions

In this study, a hybrid structural health monitoring (SHM) scheme using a parallel acceleration-impedance approach was proposed to detect girder damage and support damage in steel plate-girder bridges which are under ambient train-induced excitations. The hybrid SHM scheme consisted of

three phases: global and local damage monitoring in parallel manner, damage occurrence alarming and local damage identification, and detailed damage estimation. In the first phase, damage occurrence in a structure was globally monitored by changes in vibration features and, at the same moment, damage occurrence in local critical members was monitored by changes in impedance features. In the second phase, the occurrence of damage was alarmed and the type of damage was locally identified as either girder damage or support damage by recognizing patterns of vibration and impedance features. In the final phase, the location and severity of the locally identified damage were estimated by using modal strain energy-based damage index methods. The feasibility of the proposed scheme was evaluated on a steel plate-girder bridge model which was experimentally tested under model train-induced excitations. Acceleration responses and electro-mechanical impedance signatures were measured for several damage scenarios of girder cracks and support failures.

From the experimental evaluation, the following results were obtained. Firstly, the correlation coefficient of power spectral densities was selected for the acceleration-based global monitoring method and the root-mean-square-deviation was selected for the impedance-based local monitoring method. Secondly, the hybrid damage monitoring was mainly performed for two damage types, girder crack and support failure. For a crack in the middle of a girder, the parallel acceleration-impedance approaches successfully alarmed the occurrence and the location of damage. It also predicted the severity of girder damage in the alerted location with relatively conservative estimation. For a few support damage cases, the parallel approaches worked satisfactorily to alarm small incipient damage, which could not be monitored by vibration-based methods. It also predicted the severity of support damage in the alerted location, but the accuracy of severity estimation was relatively low. Future efforts should be focused on improving the accuracy of damage severity estimation. Also, further studies are remained to evaluate the practicality of the hybrid SHM methodology on more realistic bridges.

Acknowledgements

This work was supported by the Pukyong National University Research Fund in 2010 (PK-2010-121) and The first author was financially supported by Brain Korea 21 Program funded by Korean Ministry of Education, Science, and Technology.

References

Adams, R.D., Cawley, P., Pye, C.J. and Stone, B.J. (1978), "A Vibration Technique for Non-destructively Assessing the Integrity of Structures", *J. Mech. Eng. Sci.*, **20**, 93-100.

Bendat, J.S. and Piersol, A.G. (2003), *Engineering Applications of Correlation and Spectral Analysis*, Wiley-Interscience, New York, NY.

Bhalla, S. and Soh, C.K. (2004). "Structural Health Monitoring by Piezo-Impedance Trans-ducers II: Applications", *J. Aeros. Eng.*, **17**(4), 166-175.

Brincker, R., Zhang, L. and Andersen, P. (2001), "Modal identification of output-only systems using frequency domain decomposition", *Smart Mater. Struct.*, **10**(3), 441-445.

Catbas, F.N., Brown, D.L. and Aktan, A.E. (2006), "Use of modal flexibility for damage detection and condition assessment: case studies and demonstrations on large structures", *J. Struct. Eng. -ASCE*, **132**(11), 1699-1712.

Doebling, S.W., Farrar, C.R., and Prime, M.B. (1998), "A summary review of vibration-based damage identification methods", *Shock. Vib. Dig.*, **30**(2), 91-105.
Gao, Y. and Spencer, B.F. (2002), "Damage localization under ambient vibration using changes in flexibility", *Earthq. Eng. Eng. Vib.,* **1**(1), 136-144.
Giurgiutiu, V. and Zagrai, A.N. (2002), "Embedded self-sensing piezoelectric active sensors for on-line structural identification", *J. Vib. Acoust.*, **124**(1), 116-125.
Hong, D.S., DO, H.S., Na, W.B. and Kim, J.T. (2009), "Hybrid structural health monitoring of steel plate-girder bridges using acceleration-impedance features", *KSCE J.*, **29**(1A), 61-71.
Kessler, S.S. (2002), "Piezoelectric-based in-situ damage detection of composite materials for structural health monitoring systems", Ph.D. Dissertation, Massachusetts Institute of Technology, U.S.A.
Kim, J.T. and Stubbs, N. (1995), "Model uncertainty impact and damage-detection accuracy in plate girder", *J. Struct. Eng.*, **121**(10), 1409-1417.
Kim, J.T. and Stubbs, N. (2002), "Improved damage identification method based on modal information", *J. Sound. Vib.*, **252**(2), 223-238.
Kim, J.T., Ryu, Y.S., Cho, H.M. and Stubbs, N. (2003), "Damage identification in beam-type structures: frequency-based method vs mode-shape-based method", *Eng. Struct.,* **25**(1), 57-67.
Kim, J.T., Park, J.H. and Lee, B.J. (2007), "Vibration-based damage monitoring in model plate-girder bridges under uncertain temperaturet conditions", *Engi. Struct.*, **29**, 1354-1365.
Kim, J.T., Park, J.H., Hong, D.S. and Park, W.S. (2010), "Hybrid health monitoring of prestressed concrete girder bridges by sequential vibration-impedance approaches", *Eng. Struct.*, **32**, 115-128.
Koo, K.Y. (2008), "Structural health monitoring methods for bridges using ambient vibration and impedance measurements", Ph.D. Dissertation, Korea Advanced Institute of Science and Technology, Daejon, Korea.
Liang, C., Sun, F.P. and Rogers, C.A. (1996), "Electro-mechanical impedance modeling of active material systems", *Smart Mater. Struct.*, **5**(2), 171-186.
Ni, Y.Q., Hua, X.G., Fan, K.Q. and Ko, J.M. (2005), "Correlating modal properties with temperature using long-term monitoring data and support vector machine technique", *Eng. Struct.*, **27**, 1762-1773.
Park, G., Kabeya, K., Cudney, H.H. and Inman, D.J. (1999), "Impedance-based structural health monitoring for temperature varying applications", *JSME Int. J.*, **42**(2), 249-258.
Park, S., Yun, C.B., Roh. Y. and Lee, J. (2005), "Health monitoring of steel structures using impedance of thickness modes at PZT patches", *Smart Struct. Syst.*, **1**, 339-353.
Park, G., Farrar, C.R., Scalea, F.L. and Coccia, S. (2006), "Performance assessment and validation of piezoelectric active-sensors in structural health monitoring", *Smart Mater. Struct.*, **15**(6), 1673-1683.
Sohn, H., Farrar, C.R., Hemez, F.M., Shunk, D.D., Stinemates, D.W. and Nadler, B.R. (2003), "A review of structural health monitoring literature: 1996-2001", Los Alamos National Laboratory Report, LA-13976-MS, Los Alamos National Laboratory, USA.
Sohn, H., Farrar, C.R., Hunter, N.F. and Worden, K. (2001), "Structural health monitoring using statistical pattern recognition techniques", *ASME J. Dyn. Syst., Measur. Control*, **123**(4), 706-711.
Stubbs, N. and Osegueda, R. (1990), "Global nondestructive damage evaluation in solids", *Int. J. Anal. Exper. Mod. Anal.*, **5**(2), 67-79.
Sun, F.P., Chaudhry, Z.A., Rogers, C.A., Majmundar, M. and Liang, C. (1995), "Automated real-time structure health monitoring via signature pattern recognition", *Proceeding of SPIE Conference on Smart Structures and Materials*, Vol. 2443, San Diego, USA.
Yang, Y.B., Yau, J.D. and Hsu, L.C. (1997), "Vibration of simple beams due to trains moving at high speeds", *Eng. Struct.*, **19**, 936-944.
Yi, J.H. and Yun, C.B. (2004), "Comparative study on modal identification methods using output-only information", *Struct. Eng. Mech.*, **17**(3-4), 445-456.